Performance Analysis of Near-Space Vehicle-Borne Millimeterwave Radiometer

Wen-Qin Wang, *Member, IEEE*
1. Sch. of Comm.. Info. Eng., University of Electronic Science and Technology of China, Chengdu
2. Key Laboratory of Ocean Circulation and Waves, Chinese Academy of Sciences, Qingdao
3. State Key Laboratory of Millimeter Waves, Southeast University, Nanjing
Email: wqwang@uestc.edu.cn

***Abstract*— Near-space is recognized as the altitudes between 20 kilometer (km) and 100 km. The thinness of the atmosphere makes it difficult for satellites and airplanes to operate there. However, the vehicles operating in near-space offer several advantages over satellites and airplanes. These advantages provide potential for specific remote sensing applications. In this paper, the near-space vehicle-borne millimeterwave radiometer is designed for regional ocean remote sensing. One conceptually design system is investigated, along with the performance analysis of detection range and imaging sensitivity. It is shown that the near-space vehicle-borne millimeterwave radiometer can efficiently overcome the shortcoming of spaceborne radiometer in spatial resolution.**

I. Introduction

Passive remote sensing of the earth's surface has progressed considerably in recent years. Microwave and millimeterwave radiometers have established itself as an effective remote sensing tool for determining surface and atmospheric parameters [1]–[3]. These parameters include ocean surface temperature, salinity, windspeed, soul moisture content, and arctic sea ice concentration. Spaceborne microwave radiometers have been producing monthly-averaged large scale maps of sea ice since the 1970's [4]. However, spaceborne radiometer has a drawback of low spatial resolution, which is on the order of tens of kilometers. In fact, the measurement spatial resolution is constrained by the available antenna aperture size in the radiometer. In spaceborne radiometers a 1-m aperture allows for approximately 15-150 km spatial resolution over the frequency range 20-2 GHz. This drawback can be efficiently resolved by employing near-space vehicles as the radiometer platforms.

Near-space is recognized as the altitudes between 20-km and 100-km [5]. Note that the lower limit is not determined from operational considerations, but from the international controlled airspace altitude. The thinness of the atmosphere makes it difficult for satellites and airplanes to operate there. However, advances have opened the door for some vehicles to operate in near-space. As shown in Fig. 1, the vehicles operating in near-space offer several advantages that are not accessible for current satellites and airplanes. Generally, there are two kinds of vehicles that can fly or float in near-space. Figure 2 gives several typical near-space vehicles [6]. One kind is the free-floaters which can be further classified free-floating balloons and steered free-floaters. The flying speed and direction of free-floating balloons depend primarily on the existing winds. Free-floaters which can take tens to thousands of pounds to over 30-km have already been demonstrated commercial viability as communication platforms [7]. Steered free-floaters also drift on the winds, but they are able to exploit the winds to maneuver at will. These free-floaters can provide a persistent regional coverage that is impossible for satellites and airplanes.

The other type is the maneuvering vehicles which can use different propulsion mechanisms to fly or keep stationary over an area of interest for a long time [8]. They can provide a large footprint and a long mission that are commonly associated with satellites and the fast responsiveness of an unmanned aerial vehicle (UAV). As they are not constrained by orbital mechanics like satellites, maneuvering vehicles can move at a high speed. Additionally, when near-space vehicles fly at an altitude high enough to provide wide region coverage, they are much closer to the targets than satellites. Considering a point at nadir, near-space vehicles are 10-20 times closer to the targets than a typical 700-km LEO satellite. This distance differential implies that near-space vehicle-borne radiometer could have much higher imaging sensitivity.

Near-space thus provide a new opportunity to develop new remote sensing technique. We have investigated the near-space vehicle-borne radar for different remote sensing applications in [9]–[12]. In this paper, the near-space vehicle-borne millimeterwave radiometer is designed for regional ocean remote sensing. This paper concentrates on conceptually design and performance analysis. The remaining sections are organized as follows. Section II described the scheme of near-space vehicle-borne millimeterwave radiometer. Section III derived the corresponding radiometric performances including imaging sensitivity and detection range. This paper is concluded in Section IV.

II. Near-Space Vehicle-Borne Millimeter Radiometer

The frequency chosen for a wave and precipitation measurement radiometer carried in a spacecraft must be a compromise. Too high a frequency will result in excessive attenuation for the radiometer contribution caused by precipitation in the lower atmosphere. Too low a frequency will will require a

978-1-4244-9171-1/11/$26.00 ©2011 IEEE

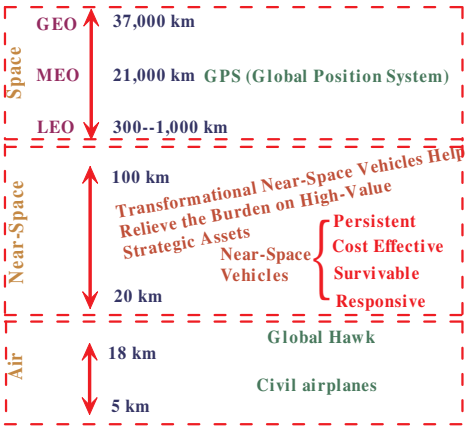

Fig. 1: Near-space definition and its advantages while compared to aerospace including geosynchronous orbit (GEO), middle earth orbit (MEO) and low earth orbit (LEO), and airspace.

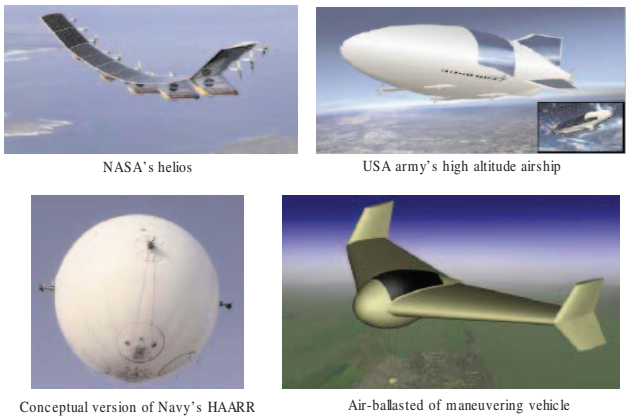

NASA's helios

USA army's high altitude airship

Conceptual version of Navy's HAARR

Air-ballasted of maneuvering vehicle

Fig. 2: Several typical near-space vehicles [6].

large antenna; moreover, low-frequency emission from precipitation will be so small that it will be difficult to measure and to separate from the variable background of sea-surface emission. As near-space vehicle has a very limited load capability and rigorous geometry constraint, this paper considers only millimeterwave radiometers.

There are several different kinds of radiometers such as Dicke-switched and noise injection radiometers, but this paper considers only total power radiometer. The total power radiometer offers the potential of providing the best sensitivity and the simplest realization of any common radiometer configuration, and thus is an attractive choice for imaging applications. As shown in Fig. 3, each near-space vehicle-borne receiver chain consists of a RF amplifier, a mixer, a local oscillator, a low-noise IF amplifier, a square-law detector, a specially designed video amplifier, and a signal conditioning section which performs both signal conditioning and integration. The radiometric power must be detected to determine its characteristics, so a tunnel diode square-law detector is usually employed because it relates output voltage to input power. Note that an attenuator is also widely applied

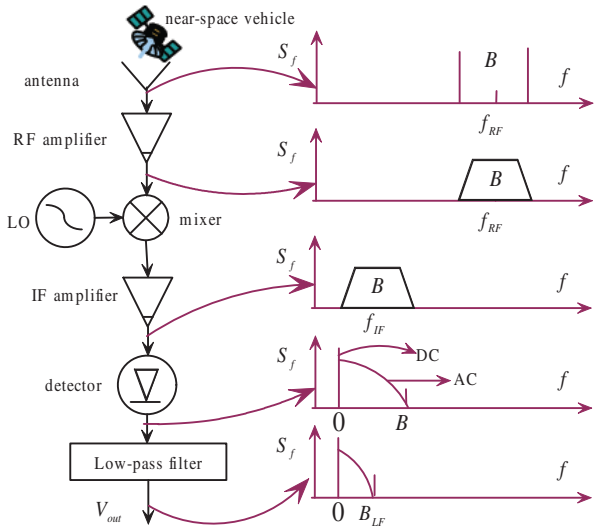

Fig. 3: Block diagram of the near-space vehicle-borne radiometer.

in the IF section to ensure that the detectors operate in a pure square law mode, as well as reducing their noise contribution. Finally, an integration device is employed to smooth the signal over some time duration and deliver a mean signal.

The radiometer maps the brightness temperature distribution over a given field of view. As the thermal emission by the earth provides an incident flux density, the power available at the antenna output terminals can be expressed as

$$P = \frac{A_r}{2} \iint_{4\pi} \frac{2K}{\lambda^2} \cdot T_{AP}(\theta, \phi) \cdot B \cdot F_n(\theta, \phi) \mathrm{d}\Omega \tag{1}$$

where A_r is the antenna's effective area, K is Boltzmann's constant, λ is wavelength, $T_A(\theta, \phi)$ is the incident brightness temperature with (θ, ϕ) is the solid angle locating the incoming direction of the emission, B is the signal bandwidth, and $F_n(\theta, \phi)$ is the directive gain pattern of the antenna. This expression can be represented by

$$P = K \cdot T_A \cdot B \tag{2}$$

where T_A is the antenna radiometric measurement temperature defined as

$$\begin{aligned} T_A =& \frac{\iint_{4\pi} T_{AP}(\theta, \phi) \cdot F_n(\theta, \phi) \mathrm{d}\Omega}{\iint_{4\pi} F_n(\theta, \phi)} \\ =& \frac{\Delta T_{AP}(\theta_F) \cdot G_0 \cdot h_s}{4\pi} \\ & \cdot \int_{x_1}^{x_2} \int_{y_1}^{y_2} \frac{exp\{-b[\cos^{-1}(\frac{h_s \cdot \cos\theta_F + y \sin\theta_F}{(h_s^2 + x^2 + y^2)^{1/2}})]^2\}}{(h_s^2 + x^2 + y^2)^{3/2}} \mathrm{d}x\mathrm{d}y \end{aligned} \tag{3}$$

where ΔT_{AP} is the target's temperature while compared to the calibration temperature, G_0 is the gain of the antenna with the waveform coefficient of b, θ_F is the antenna incident angle, h_s is the receiver's altitude, and (x, y) is the target's position.

As an example, suppose $\Delta T_{AP} = 50K$, $G_0 = 1500$, $h_s = 5000m$, $x_1 = -3m$, $x_2 = 2m$, $y_1 = 45m$, $y_2 = 50m$ and $b = 400$,

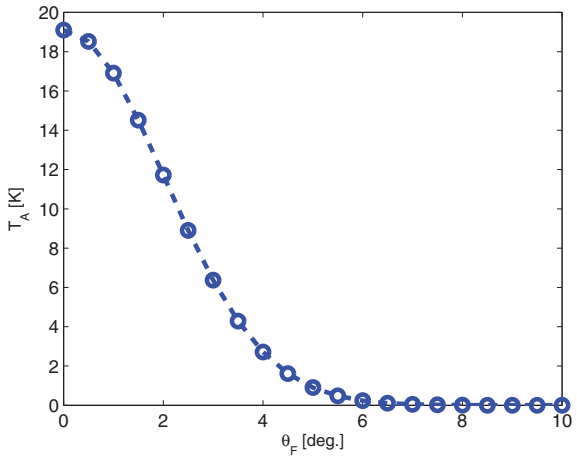

Fig. 4: Example measurement temperature as a function of θ_F.

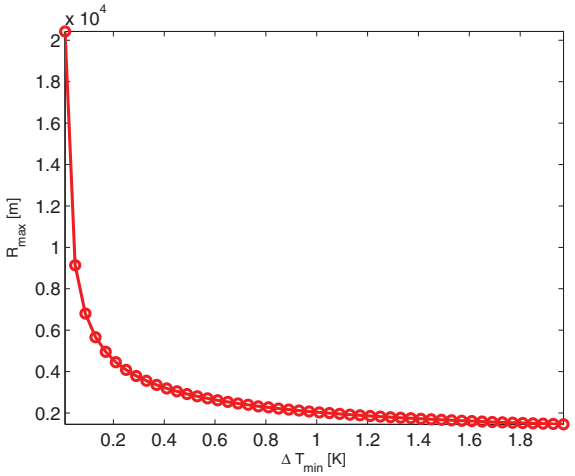

Fig. 5: The imaging range as a function of detection sensitivity.

Figure 4 gives the corresponding T_A as a function of the θ_F. It can be noticed that near-space vehicle-borne millimeterwave radiometer is possible for remote sensing applications.

The objective of radiometry is just to measure the brightness temperature of objects. The near-space vehicle-borne receiver selects a certain portion of the power, T_A, delivered by the antenna, characterized by a bandwidth, B, amplifies it with a gain G, and feeds it to an output device. However, in this process the receiver also generates noise, T_{noise}. Both the signal and noise signals will be summed in the receiver. The noise signal consists of a mean part and a fluctuating part. The mean part may be removed duration subsequent calibration processing, while the fluctuating part remains part of T_{sys} and cannot be separated later. Therefore, there is

$$P = K \cdot B \cdot (T_A + T_{noise}) = K \cdot B \cdot T_{sys} \tag{4}$$

The output signal at the square-law detector can then be represented by

$$V_d = \alpha^2 \cdot C_d \cdot K \cdot T_{sys} \cdot B \tag{5}$$

where α and C_d are the voltage gain of the receiver and the power sensitivity of the square-law detector, respectively. Therefore, the final output of the filter is

$$V_{out} = g_{LF} \cdot \alpha^2 C_d \cdot K \cdot (T_{AP}(\theta_0, \phi_0) + T_{noise}) \cdot B \tag{6}$$

where g_{LF} is the direct current gain of the low-pass filter. The radiometric image can then be obtained by combining the V_{out} at different (θ, ϕ). z

III. Performance Analysis

The sensitivity of the total power radiometer is often expressed by [13], [14]

$$\Delta T_{min} = T_{sys} \cdot \sqrt{\frac{1}{B \cdot \tau} + (\frac{\Delta G}{G})^2} \tag{7}$$

where τ is the equivalent postdetection integration time, and the quantity $\Delta G/G$ represents the normalized rms fluctuation of the receiver power gain. Note that this expression fails to account for the effects of noise in radiometer calibration measurements. Considering the signal-to-noise ratio (SNR) of the total power radiometer

$$\frac{S}{N} = (\frac{2\Delta T_A}{2T_{sys}})^2 \cdot \frac{B_{IF}}{2B_{RF}} \tag{8}$$

where B_{IF} and B_{RF} denote the RF amplifier bandwidth and IF amplifier bandwidth, respectively. The detection range of the radiometer can then be expressed as [15]

$$R = \sqrt{\frac{\eta \cdot A_T \cdot \Delta T_T \cdot \pi \cdot \eta \cdot D^2}{\lambda^2 \cdot \Delta T_{min} \sqrt{S/N}}} \tag{9}$$

where η is the antenna coefficient, A_T is the target's effective area, D is the antenna diameter, ΔT_T is the comparative target radiometric temperature equal to

$$\Delta T_T = \frac{\Delta T_A \cdot \Omega_A}{\eta \cdot \Omega_T} \tag{10}$$

with Ω_A and Ω_T the antenna solid angle and target solid angle respectively.

As an example, suppose $\eta = 0.8$, $A_T = 25$, $\Delta T_T = 50$, $\lambda = 0.008m$, $D = 2m$ and $S/N = 1$, Figure 5 gives example maximum imaging ranges as a function of the detection sensitivity, ΔT_{min}. It can be noticed that the detection range will be impacted by the antenna diameter and radiometer operational frequency. The detection range can be extended by increasing antenna diameter and/or operational frequency. To obtain a longer imaging range, large antennas are usually employed in current spaceborne radiometers. However, scanning of the narrow antenna beam is a potential problem. Moreover, the dwell time available on each pixel of a high-resolution pencil beam scanning will be insufficient to produce satisfactory data.

To extend the detection range, synthetic aperture can be employed in the radiometer. Figure 6 illustrates the near-space vehicle-borne synthetic aperture radiometer. For the synthetic

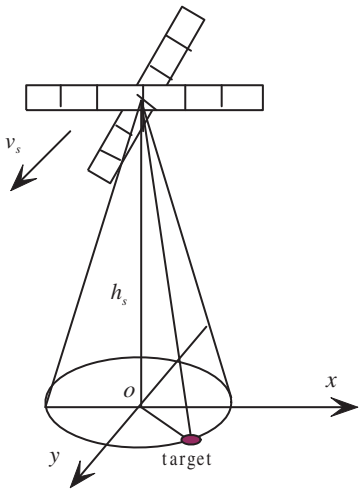

Fig. 6: Several typical near-space vehicles [6].

aperture radiometer, its imaging sensitivity is determined by [16]

$$\Delta T'_{min} = T_{sys} \cdot N^{3/2} \cdot \sqrt{V \cdot d_x/(2B \cdot R \cdot \lambda)} \tag{11}$$

where N is the number of array elements in the azimuth direction with element space of d_x, and V is the visibility function. The corresponding maximum detection range is

$$R_{max} = \sqrt{[\frac{N \cdot B \cdot \lambda \cdot \Delta T_T^2 \cdot G^2 \cdot A_r^2}{8v_s \cdot d_x \cdot T_{sys}^2 \cdot \pi^2}]^3} \tag{12}$$

In this case, a maximum detection range of $5km$ can be obtained the synthetic aperture radiometer with about 200 array elements in the azimuth direction.

IV. Conclusion

Near-space vehicles can provide a remote sensing platform that is more responsively and more persistently than satellites and airplanes for several reasons. Firstly, it can support uniquely effective and economical operations. Secondly, it enables a new class of especially useful remote sensing tool. And finally, it provides a crucial corridor for prompt regional strike. This paper describes one near-space vehicle-borne millimeterwave radiometer for regional ocean remote sensing. The conceptually design system is investigated.

Note that near-space vehicle-borne radiometers cannot replace spaceborne and airborne radiometers, but they could provide remote sensing functionality similar to spaceborne radiometers more efficiently than the former ones. Although near-space vehicles have much smaller imaging coverage area than that of satellites due to their lower operational altitude, they can still offer a regional coverage of hundreds of kilometers and provide cost-effective remote sensing services. Near-space vehicle-borne radiometers could also extend remote sensing services into areas with limited or no access to spaceborne and/or airborne radiometers, e.g., ocean remote sensing. Therefore, given their operational flexibility, near-space vehicle-borne radiometers would supply a gap between spaceborne and airborne radiometers.

One remaining problem is the required motion compensation for near-space vehicle-borne radiometers, particularly for synthetic aperture radiometers. In current spaceborne and airborne sensors, global positioning system (GPS) receiver and inertial navigation system (INS) are usually employed for this task. But, for near-space vehicle-borne sensors, motion measurement facilities may be not reachable because of its limited load capabilities.

ACKNOWLEDGEMENTS

This work was supported in part by the open funds of the State Key Laboratory of Millimeter Waves under contract number *200914*, and the Key Laboratory of Ocean Circulation and Waves, Chinese Academy of Sciences under contract number *KLOCAW1004*.

References

[1] B. Collins, F. G. R. Warren, and J. L. Paul, "Airborne imaging microwave radiometer-part I: radiometric analysis," *IEEE Trans. Geosci. Remote Sens.*, vol. 34, no. 3, pp. 643–655, May 1996.

[2] R. Bernard, A. L. Cornec, L. Eymard, and L. Tabary, "The microwave radiometer aboard ERS-1: part 1-characteristics and performances," *IEEE Trans. Geosci. Remote Sens.*, vol. 31, no. 6, pp. 1186–1198, Nov. 1993.

[3] B. Guner, J. T. Johnson, and N. Niamsuwan, "Time and frequency blanking for radio-frequency interference mitigation in microwave radiometry," *IEEE Trans. Geosci. Remote Sens.*, vol. 45, no. 11, pp. 3672–3679, Nov. 2007.

[4] R. P. Moore, and M. C. Hooper, "An airborne Ka-band microwave radiometric measurement mapping system," *Proc. SPIE*, vol. 27, pp. 147–156, 1971.

[5] E. H. Allen, "The case for near-space," *Aerospace America*, vol. 22, no. 1, pp. 31–34, Mar. 2006.

[6] E. B. Tomme, "Balloons in today's military: an introduction to near-space concept," *Air Space Journal*, vol. 19, no. 4, pp. 39–50, April 2005.

[7] M. J. Marcel, and J. Baker, "Interdisciplinary design of a near-space vehicle," *Proc. of Southeast Conf.*, Richmond, USA, 2007, pp. 421–426.

[8] G. Rome, and G. Frulla, "HELIPLAT: high altitude very-long endurance sonar powered UAV for telecommunucation and earth observation applications," *Aeronautical Journal*, vol. 108, no. 3, pp. 277–293, Jun. 2004.

[9] W. Q. Wang, "Application of near-space passive radar for homeland security," *Sens. Imag. An Int. J.*, vol. 8, no. 1, pp. 39–52, Mar. 2007.

[10] W. Q. Wang, J. Y. Cai, and Q. C. Peng, "Near-space SAR: a revolutionizing remote sensing mission," *Proc. of Asia-Pacific Synthetic Aperture Radar Conf.*, Huangshan, China, vol. 2007, pp. 127–131.

[11] W. Q. Wang, J. Y. Cai, and Q. C. Peng, "Near-space microwave radar remote sensing: potentials and challenge analysis," *Remote Sens.*, vol. 2, no. 3, pp. 717–739, Mar. 2010.

[12] W. Q. Wang, "Near-space wide-swath radar imaging with multiaperture antenna," *IEEE Antenna Wireless. Propag. Lett.*, vol. 8, pp. 461–464, Nov. 2009.

[13] M. S. Hersman, and G. A. Poe, "Sensitivity of the total power radiometer with periodic absolute calibration," *IEEE Trans. Micro. Theory Tech.*, vol. 29, no. 1, pp. 32–40, Jan. 1981.

[14] J. C. Bremer, "Improvement of scanning radiometer performance by digital reference averaging," *Microwaves*, vol. 17, no. 9, pp. 64–74, Sept. 1978.

[15] X. G. Li, and Y. H. Li, *Millimeterwave Near-Field Sensing Technique Basics*, (in Chinese), Beijing Institute of Technology Press, 2009.

[16] L. Lang, Z. Y. Zhang, W. Guo, and F. Hu, "Performance analysis of application of airborne synthetic aperture radiometer to target detection," *J. Huazhong Univ. of Sci. & Tech.*, (Natural Science Edition), (in Chinese), vol. 36, no. 10, pp. 59–62, Oct. 2008.